ELSEVIER

Journal of Nuclear Materials 290–293 (2001) 892–895

journal of nuclear materials

www.elsevier.nl/locate/jnucmat

Impurity radiation modulations in an ergodic divertor

F. Laugier *, M. Bécoulet, C. De Michelis, Ph. Ghendrih, J.P. Gunn, P. Monier-Garbet, R. Reichle, J.C. Vallet

Association Euratom–CEA, DRFC, CEA Cadarache, Bat. 513, 13108 St Paul lez Durance, France

Abstract

The 3-D geometry of radiation losses is investigated in the Tore Supra ergodic divertor. Measurements from passive bolometers located on the divertor coils show evidence of toroidal and poloidal radiation modulations. They were interpreted using a 3-D code solving heat transport equation that gives the whole geometry of plasma radiation in a divertor configuration close to Tore Supra. The results of the code are in qualitative agreement with the measurements and they show that the total radiated power is underestimated when inferred from standard bolometers located between divertor modules. Maximum of radiation in front of the modules is explained by the multiplication of radiative zones at this place due to the intersection of field lines with the vessel wall. This effect leads to non-monotonic temperature profiles along field lines in the boundary plasma.

Keywords: Divertor radiation; Passive bolometer; Temperature profile

1. Introduction

Power load on the divertor target plates cannot exceed a technological limit, estimated between 5 and 20 MW m^{-2}, in long time shots. As a consequence, plasma power deposition needs to be balanced with impurity radiation in the boundary plasma. In Tore Supra, the radiation loss capability is studied in the ergodic divertor configuration. The resonant magnetic perturbation, with poloidal and toroidal main numbers $\bar{m} = 18$ and $\bar{n} = 6$, generates a 3-D magnetic structure. In this paper, we focus on the radiation inhomogeneities in order to estimate the exact radiation capability of the ergodic divertor. Calorimetric measurements have already shown that radiation is maximum in front of the divertor modules [1]. Thus the total radiation could be underestimated when inferred from diagnostics located between divertor modules, such as standard bolometry. New results from passive bolometers set on divertor coils show evidence of radiation modulations in poloidal and toroidal directions. These modulations were simulated using a 3-D code solving heat transport equation in the stochastic field of the ergodic divertor.

2. Experimental results

Passive bolometers are orthotropic pyrocarbon tiles set back from the wall protections so that they are out of reach of plasma conducted or convective heat fluxes. The temperature increase of these bolometers is only due to incident impurity radiation flux and due to collisions with charge exchange neutrals. The temperature increase is measured by an infrared camera watching the divertor. Then the incident radiation flux is computed using a 1-D code that evaluates heat propagation through the pyrocarbon tile. Passive bolometers are set on divertor coils (see Fig. 1 left) allowing measurements in inaccessible places for standard bolometry with better resolution.

In Fig. 1, we compare the radiated power given by standard bolometers P_{rad} and the incident flux F_{PB} on passive bolometers PB_s, Fig. 1 middle, and PB_m, Fig. 1 right. PB_m is set on the middle of the divertor and PB_s at its side. P_{rad} and F_{PB} are plotted as a function of time for

* Corresponding author. Tel.: +33-442 254 025; fax: +33-442 254 990.

E-mail address: laugier@pegase.cad.cea.fr (F. Laugier).

0022-3115/01/$ - see front matter
PII: S0022-3115(00)00541-9

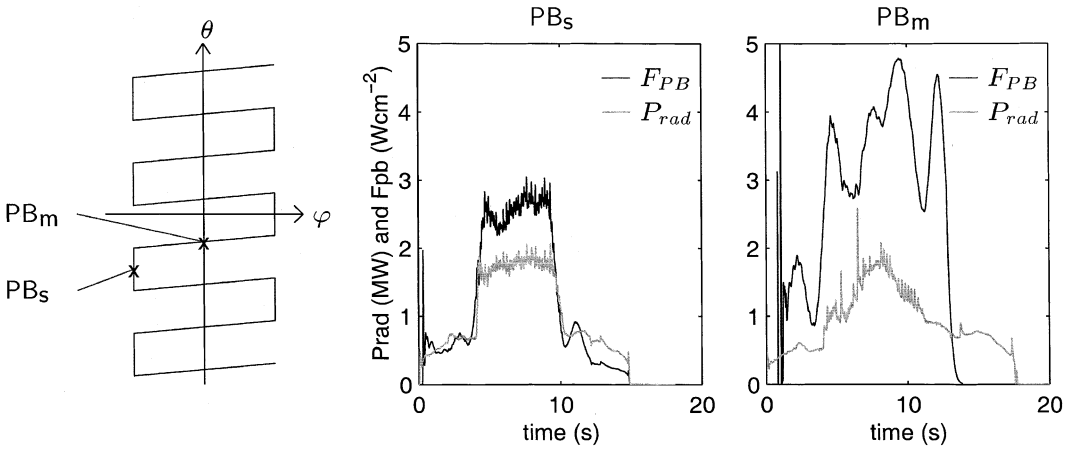

Fig. 1. Left: position of passive bolometers PB_m and PB_s on the divertor module. Middle: radiated power measured by standard bolometers P_{rad} and incident power flux on PB_s, F_{PB}, as a function of time during shot 28068. Right: P_{rad} and F_{PB} for PB_m as a function of time during shot 28219.

similar shots with nitrogen injection and 4 MW ion cyclotronic radiofrequency heating. At the same value of $P_{rad} = 1.8$ MW, corresponding to an incident flux given by standard bolometers, $F_{SB} = 2.4 \times 10^{-2}$ MW m^{-2}, the measured value of incident flux for PB_s is $F_{PB_s} = 2.8 \times 10^{-2}$ MW m^{-2}, and for PB_m, $F_{PB_m} = 3.8 \times 10^{-2}$ MW m^{-2}. We observe modulations of the incident fluxes but we cannot decide whether they are due to impurity radiation modulations or charge exchange neutral flux modulations. The comparison between radiation measurements with standard and passive bolometers is further complicated by the sensitivity to charge exchange neutrals one expects for the passive bolometers. Indeed, the standard bolometers view the recycling areas through the plasma that is opaque to neutrals.

3. 3-D model

3.1. Model

In order to simulate radiation modulations, we need to compute the temperature field $T(r, \theta^*, \varphi)$ in the stochastic field of the divertor. θ^* and φ are intrinsic magnetic coordinates associated with the ergodic divertor such as $d\varphi/d\theta^* = q$. Temperature is determined by solving in 3-D the energy conservation equation

$$\partial_t\left(\frac{3}{2}nT\right) = \left(\vec{\nabla}_{//} + \tilde{\vec{\nabla}}_{//}\right)\left[n\chi_{//}(\vec{\nabla}_{//} + \tilde{\vec{\nabla}}_{//})T\right] + \vec{\nabla}_{\perp}(n\chi_{\perp}\vec{\nabla}_{\perp}T) - n^2 c_z F_R(T), \quad (1)$$

where $n = 10^{19}$ m^{-3}, the plasma density, and $c_z = 1\%$, the impurity concentration, are constant. The parallel conductivity is $n\chi_{//} = \kappa_0 T^{5/2}$ with $\kappa_0 = 2 \times 10^{22}$ m^{-1} s^{-1}, T in eV. The perpendicular diffusivity is $\chi_{\perp} = 3$ m^2 s^{-1}. The unperturbed gradients, corresponding to the magnetic equilibrium without the ergodic divertor, are $\vec{\nabla}_{//} = \vec{e}_B/R_{tor}(-1/q\,\partial_{\theta^*} + \partial_{\varphi})$ and $\vec{\nabla}_{\perp} = \vec{e}_r\partial_r + \vec{e}_{\theta^*}/r\partial_{\theta^*}$, where $\vec{e}_B$, $\vec{e}_r$ and $\vec{e}_{\theta^*}$ are unitarian vectors in unperturbed magnetic field $\vec{B}$, r and θ^* the directions, $R_{tor} = 2.38$ m the major radius of the tokamak, and the safety factor q is proportional to r^2.

Perpendicular heat transport is enhanced by parallel transport typically along the radial magnetic perturbation via the perturbed parallel gradient $\tilde{\vec{\nabla}}_{//} = (\delta\vec{B}_r/B)\partial_r$. Eq. (1) is solved in the Fourier space associated with θ^* and φ coordinates. Poloidal and toroidal main modes of the perturbation are similar to those of the ergodic divertor of Tore Supra. In the simulation, the perturbation is symmetric in θ^* and φ, in order to minimize the number of modes. Close to the wall, the radial perturbation is exponentially decreasing with r. The perturbation spectrum is the Fourier transformation of $\delta(\Delta\varphi)\delta(\Delta\theta^*)\sin\bar{m}\theta^*$ where δ is a gate function and $\Delta\varphi$ and $\Delta\theta^*$ are the toroidal and poloidal extension of modules, respectively, the toroidal period being $2\pi/6$. We obtain sine cardinal functions, centered on modes $k\bar{n} = 0$, $m = \bar{m}$ and $m = -\bar{m}$, see [2] and [3]. At a radial position r such as $q(r) = m/(k\bar{n})$, the $(m, k\bar{n})$ mode is resonant. Coupling of modes is possible through the cross product of parallel gradients in Eq. (1). Far from the edge, the resonant modes with smallest $k\bar{n}$ also determine the poloidal and toroidal geometry.

The radiation function $F_R(T) = \bar{F}_R \exp[((T - T_{max})/\delta T)^2]$ stands for plasma heat losses by impurity radiations, where $T_{max} = 30$ eV, $\delta T = 10$ eV and $\bar{F}_R = 10^{-31}$ W m^3. These parameters are relevant for carbon impurities in non-equilibrium conditions [4].

The incoming perpendicular flux from the plasma center is fixed $Q_{\perp}(r_{min}) = 7.4 \times 10^3$ W m^{-2}. At the

other side, $r = a$, heat fluxes are deposited on surfaces where the magnetic radial perturbation is maximum, i.e. on neutralisers. These surfaces are connected to more inner plasma regions via open field lines. Thus we impose, as a boundary condition, that temperature is higher on neutralisers. The temperature field at $r = a$ is proportional to the magnetic radial perturbation in absolute value, $(\delta T/T)_a \propto |\delta B_r/B|_a$. The main poloidal mode relevant to our boundary conditions is also $\bar{m}_a = 36$.

3.2. Numerical analysis

Symmetries of the perturbation allow to compute only positive modes. The perturbation and boundary conditions are well simulated with $(m, k\bar{n})$ modes such as $0 \leqslant m \leqslant 50$ and $0 \leqslant k \leqslant 4$. The radial dependence of the radiation, with e-folding length of the order of 0.1 m, imposes to compute 100 points between $r_{\min} = 0.35$ m and $a = 0.8$ m. High $k\bar{n}$ modes are filtered by an additional term of numerical diffusion, introduced in Eq. (1): $D_{\text{num}}(1/R^2)\partial_{\varphi^2} T$. The numerical diffusivity is $D_{\text{num}} = (\pi R_{\text{tor}}/\Delta r k_{\max} \bar{n})^2 \kappa_{\text{erg}}$ where Δr is the radial step and $\kappa_{\text{erg}} = Q_\perp/\partial_r T$ is the effective physical diffusivity. The Eq. (1) is solved by an implicit relaxation method. In finite differential form the equation is

$$n\frac{T^{t+\Delta t} - T^t}{\Delta t} = \mathbf{A}T^{t+\Delta t} - n^2 c_z F_{\text{R}}(T^t). \tag{2}$$

Here n is the plasma density and $\mathbf{A}$ is a 25500×25500 matrix. To simplify the writing of $\mathbf{A}$, mode coupling with parallel conductivity is neglected, thus the conductivity is computed with the main mode temperature T_{00}. To obtain $T^{t+\Delta t}$, $F_{\text{R}}(T^t)$ is decomposed in the associated Fourier space.

3.3. Results

The solution of the equation is a modulated temperature field. In Fig. 2 left, the $m = 36$ mode due to boundary conditions dominates from the edge to $r = 0.79$ m. Down to $r = 0.72$ m, there is a region with island-like structures due to the mixing of hot and cool field lines in the ergodic zone. Then the resonant $m = 18$, $n = 6$ mode dominates until the perturbation is dissipated. In Fig. 2 right, the temperature is calculated along a vertical moving Langmuir probe. Its trajectory is $r\cos\theta = r_0$, θ being the real space poloidal coordinate. It is plotted in the left figure. The temperature profile is similar to experimental data, with larger temperature peaks [5].

The criterion to evaluate divertor radiation capability is the radiated power fraction along small radius,

$$f_{\text{rad}} = \frac{1}{Q_\perp(r_{\min})}\int n^2 c_z F_{\text{R}}(T)\,\mathrm{d}r. \tag{3}$$

In Fig. 3 up, f_{rad} is plotted as a function of θ^* for $\varphi = 0$. We observe radiation modulations with maxima not just above neutralisers because of the competition between the $m = 36$ mode imposed by boundary conditions and the resonant $m = 18$ mode. Poloidal structures have a characteristic length of 0.05 m in the midplane and they are located near the boundary end in front of the divertor modules. So they can be detected only by passive bolometers. Equivalent places of passive bolometers were plotted in the same figure, the ratio of radiated power incident on PB_m and PB_s is 1.28. This is in qualitative agreement with experimental result $F_{\text{PB}_\text{m}}/F_{\text{PB}_\text{s}} = 1.36$. As the impurity density nc_z increases, radiation losses increase, and for the same boundary limits, i.e. $Q_\perp(r_{\min}) = \kappa_\perp \partial_r T$ constant, $T(r_{\min})$ decreases. The temperature region where plasma can radiate moves

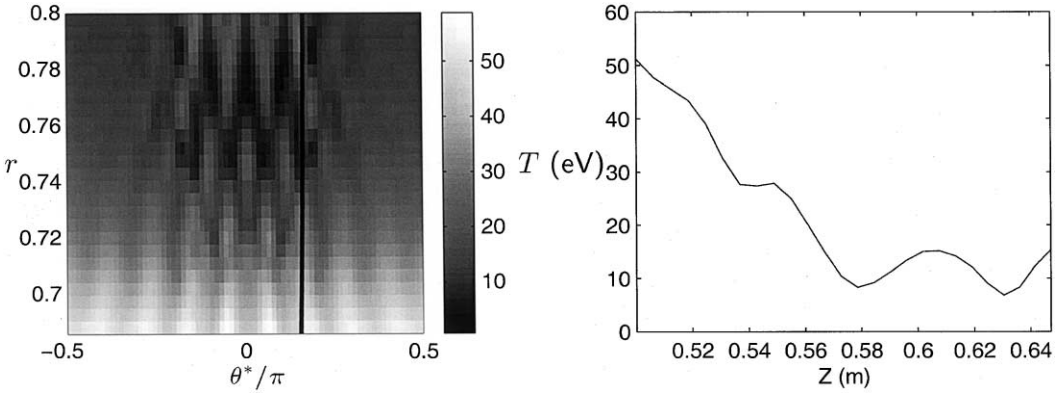

Fig. 2. Left: $T(r,\ \theta^*)$ for $\varphi = 0$, i.e. in the middle of a module. The simulated probe trajectory is drawn in black. Right: temperature profile along the probe trajectory.

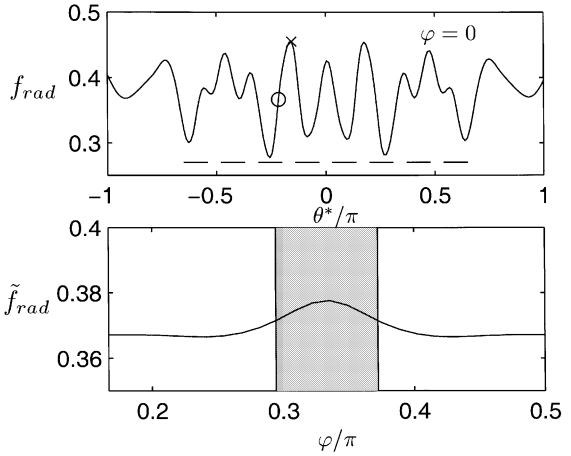

Fig. 3. Up: radiated power fraction as a function of poloidal coordinate at $\varphi = 0$, i.e. at the middle of a divertor module. '×' gives the equivalent place of passive bolometer PB_m and '○' the equivalent place of PB_s. Dashes indicates the poloidal positions of neutralisers. Down: averaged radiated fraction in poloidal direction as a function of φ. The position of the divertor is in gray.

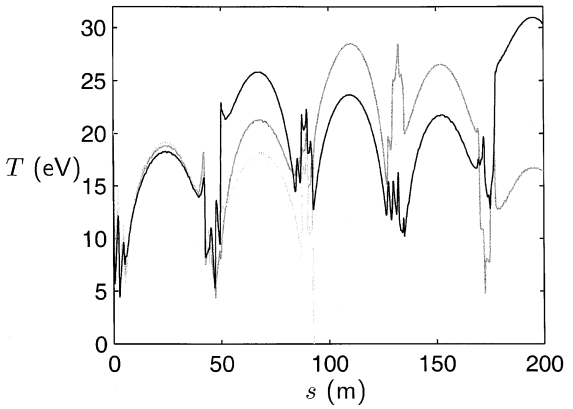

Fig. 4. Temperature profiles along field lines. Field lines are computed from initial points: $r_0 = a$, $\varphi_0 = 0$ and, from the brightest to the darkest curve, $\theta_0^* = 0.25$, $\theta_0^* = 0.26$ and $\theta_0^* = 0.27$.

inward and goes out of the ergodic zone. As a consequence, radiation modulations are attenuated when impurity density increases.

In Fig. 3 down, $\tilde{f}_{\mathrm{rad}}$ the mean radiated power on a toroidal plane is plotted as a function of φ. Radiation is maximum on the divertor module because of the boundary conditions. The $m = 36$ mode dominant in front of the modules increases the size of zones where radiation occurs. In our simulation, the effect is small because the $m = 36$ mode is rapidly attenuated. The modulation should be amplified by the condensation effect. At constant plasma pressure along a field line, a decrease of the temperature will lead to a local density increase and an enhancement of radiation. The 15% radiation modulation obtained in the present simulation without the condensation effect is therefore a minimum. Improving the density field should allow us to be closer to the 100% modulation estimated for the experimental data [1]. Since radiation appears to peak at the location of the divertor modules, standard bolometers located between divertor modules measure a region of low radiation. Another consequence is that temperature along a field line is non-monotonic as can be seen in Fig. 4. The strong dependence on initial point is due to the stochastic behaviour of field lines. For the brightest curve, temperature falls to 0 because the field line is connected back to the vessel wall. At each passage in front of the modules, the effects of radiation enhancement and mixing of field lines lead to temperature decrease.

4. Conclusion

We obtained qualitative agreement between our 3-D code and experimental results from passive bolometers set on divertor coils and a vertical moving Langmuir probe. Results from the code give the whole geometry of radiation for a divertor configuration close to the Tore Supra ergodic divertor. Also, simulations show that radiation is maximum in front of divertor modules and temperature profile along open field lines are non-monotonic. There are two consequences for the experiment. First, comparison of raw data from bolometers and the 3-D code proves that passive bolometers are not only sensitive to collisions with charge exchange neutrals. Second, the total radiated power when inferred by standard bolometers situated between divertor modules is underestimated.

References

[1] R. Reichle, J. Vallet, V. Basiuk, M. Chantant, R. Giannella, R. Guirlet, R. Mitteau, in: Proceedings of the 26th EPS Conference on Controlled Fusion and Plasma Physics, Maastricht, 1999, p. 973.
[2] P. Ghendrih et al., Tore Supra team, Progress in ergodic divertor operation on Tore Supra, Rapport bleu EUR–CEA–FC–1675, CEA–Euratom, 1999.
[3] M. Bécoulet, P. Ghendrih, H. Capes, A. Grosman, in: Proceedings of the 1999 EPS Conference on Plasma Physics and Controlled Fusion, Maastricht, 1999, p. 989.
[4] F. Laugier, P. Ghendrih, Plasma Phys. Controlled Fus. 42 (2000) 317–326.
[5] J. Gunn, P. Ghendrih, A. Grosman, F. Laugier, B. Meslin, J.-Y. Pascal, in: Proceedings of the XXVth European Conference on Controlled Fusion and Plasma Physics, vol. 22C, Prague, 1998, p. 19.